On the conditions for the occurrence of crystal avalanches during alloy solidification

Journal of Physics: Conference Series **2766** (2024) 012199 doi:10.1088/1742-6596/2766/1/012199

On the conditions for the occurrence of crystal avalanches during alloy solidification

G Shayesteh[1], A Ludwig[1], M Stefan-Kharicha[1], M Wu[1] and A Kharicha[2]

[1]Department Metallurgy, Montanuniversity Leoben, Austria
[2]Christian-Doppler Laboratory for Magnetohydrodynamic Application in Metallurgy, Montanuniversity Leoben, Austria

E-mail:golshan.siyahatshayesteh@unileoben.ac.at

Abstract. Experimental studies on the solidification of ammonium-chloride-water alloys in relatively large containments reveal conditions that lead to the formation of numerous crystal avalanches. Columnar segments that occasionally slide downwards along a vertical mushy zone further fragmentate and so crystal multiplication occurs. As a condition for this phenomenon solidification-induced solutal buoyancy that leads to a rising interdendritic flow was identified for the present case. The interaction with sedimentation-induced downward flow ahead of a vertical columnar region results in a redirection of the interdendritic flow and thus, to local conditions that slow down further solidification or even lead to remelting. Gravity is then pulling loose segments downwards. In larger containment, the flow in the bulk melt is generally unsteady and even turbulent. Thus, the outlined flow-solidification/melting interplay happens frequently at numerous positions but in a stochastic manner.

1. Introduction

In the interior of a casting, equiaxed crystals form by either heterogeneous nucleation [1-2] or fragmentation of dendrites from the columnar zone [3-5]. In regards to the last mechanism, sometimes terms like crystal multiplication [6], crystal showering [7], raining [8], or snowing [9] have been used. In 2017 the present authors reported about the observation of crystal avalanches [10], namely sliding down and subsequent fragmentation of columnar dendritic mushy zone segments that lead to thousands of crystals/fragments which then further behaves like equiaxed crystals. It was suggested that such a mechanism might also be active during the solidification of steel ingots, as periodically appearing mushy segments collapsing and corresponding crystals 'rolling down' were also reported in [11]. It is thus conceivable that crystal avalanches originated by the sliding down of mushy zone segments also contribute to the occurrence of V-segregation in centre regions of big steel ingots.

In this paper, we report on an experimental study that was performed to quantify conditions necessary for the occurrence of such crystal avalanches using ammonium chloride water as a 'model alloy' [12]. Details on the definition of the four stages that occur during the solidification process are given in [13] and on the performed Particle-Image-Velocity (PIV) measurements are given in [14]. Here, the general experimental strategy is outlined and example results are presented that are different but similar from those in [12-14]. The conclusions drawn here are justified however by the full spectrum of performed studies [12].

2. Experimental procedure

A preheated containment of relatively large size, with internal dimensions of 0.6 m in height, 0.4 m in width, and 0.06 m in depth, was filled with a solution of 29.57 wt. pct. ammonium chloride in distilled water. The containment's lateral walls and the bottom plate were constructed from brass, while the front and back walls were composed of commercial plexiglass (Polymethylmethacrylate) plates. During the experiment, the top of the containment was covered. Cooling was done from the two lateral brass walls. Water was pumped through the brass at a predefined temperature through flow channels that revealed a meandering path. As a result, a homogenous cooling of the lateral walls with a given cooling rate was achieved. This was done until a final temperature of T_{inf} = 278 K (5°C) was reached; a temperature where humidity condensation at the plexiglass windows did not occur. The disadvantage of this end temperature for cooling is that the solution in the containment never solidifies completely as the eutectic temperature of the ammonium chloride water system is at T_e = 258 K (-15°C).

Figure 1 shows the signal from six thermocouples placed at different locations in the brass sidewalls. The different readings were quite similar, revealing a homogeneous temperature distribution in the lateral walls. The final temperature was reached at approximately 5800 s after starting cooling. The curve labelled in figure 1 with G was taken inside the solution right at the centre, and the one labelled with H was taken outside the containment in direct contact with the plexiglass at a location that is close to position G. Filling of the containment was done with a solution at T_0 = 333 K (60°C) and with preheated lateral walls also at T_0. The plexiglass windows were approximately at room temperature. Cooling was started a couple of minutes after filling the containment. During this short period, the solution at position G has already cooled down by 1-2 K and the plexiglass window at position H has warmed up by 22-23 K. After approximately 3250 s after starting to cool, the temperatures at position G and H become very close.

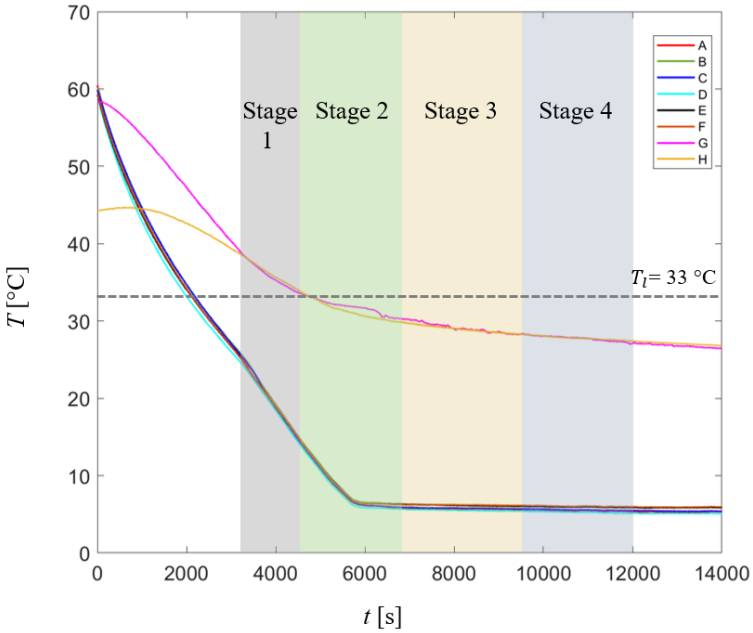

Figure 1. Six cooling curves were taken at the brass sidewalls (A-F), and two at the centre (G-H); one within the containment (G) and one outside in contact with the plexiglass window (H). The explanation for the different stages is given in the text.

As indicated in figure 1, the solidification process inside the containment happened in four different stages:

- Stage 1: 'Nucleation and growth' stage, 3250 – 4500 s
- Stage 2: 'Corner sedimentation' stage, 4500 – 6800 s

- Stage 3: ‘Swinging of turbulent snowing’ stage, 6800 – 9500 s
- Stage 4: ‘Stratified double-diffusive convection’ stage, 9500 – 12000 s

During stage 2 equiaxed crystal sediment along the columnar layers that cover the lateral walls and form crystals pileups at the left and right corner regions of the containment. During stage 3 this sedimentation process becomes unsteady, vortices occur, crystals are also carried upwards and their movement at both halves of the containment is no longer independent from each other. Predominantly at this stage, sliding down of columnar segments was frequently observed. Further details on the definition of the different stages can be found in [13].

To get quantitative data on the flow and the crystals' motion, a two-camera Particle Image Velocimetry (PIV) system with a double-pulsed solid-state Nd-YAG laser, two CCD cameras, a synchronization unit, and processing software were utilized. Two simultaneous images were captured using two distinct cameras: the first camera exclusively recorded laser light through a green filter, enabling tracking of the crystals' paths (figure 2b) Meanwhile, the second camera employed an orange filter to record solely the waves emitted by the fluorescent tracer particles, allowing for the recording of the liquid velocity field (figure 2a) Images were taken every 60 seconds, with a 1-second interval as given by the double-pulsed laser, allowing the capture of motion variations in the flowing media. Further details on the PIV measurements are given in [14].

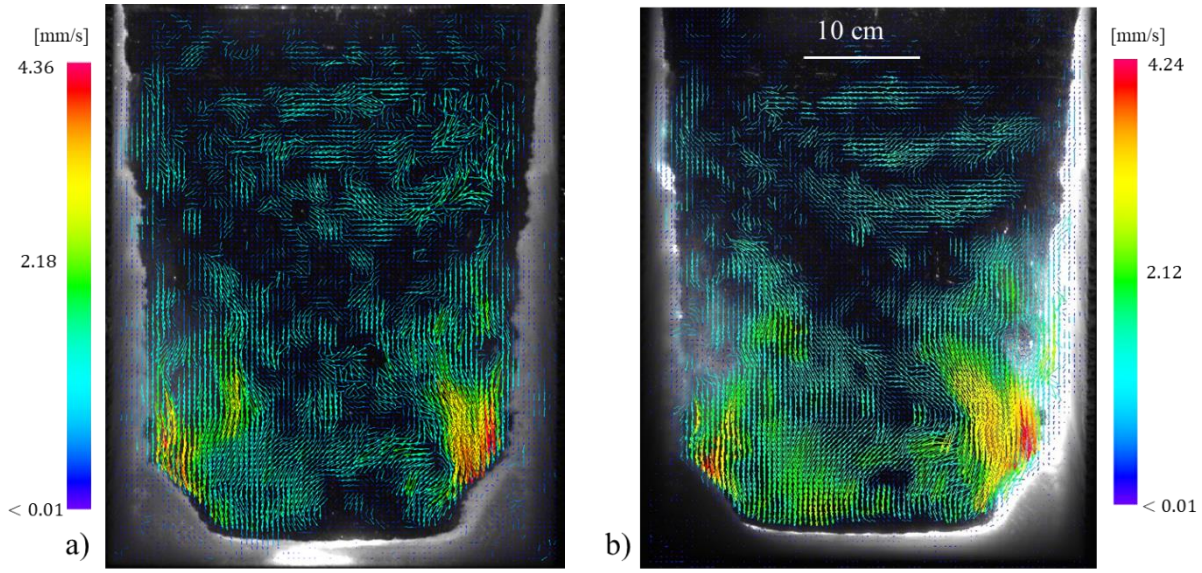

Figure 2. Example of PIV measurements performed at the beginning of stage 3 at 6800 s after the start of cooling. a) shows the velocity field of the tracers/liquid (orange filter) with v_{max} = 4.36 mm/s, and b) shows the velocity field of the equiaxed crystals (green filter) with v_{max} = 4.24 mm/s.

3. Results and Discussions

Solidification began at approximately 3250 s after starting to cool by heterogenous nucleation in direct contact with the lateral brass sidewalls (stage 1). Soon after the brass walls were completely covered with a columnar layer, equiaxed crystals were visible, especially in the two corner regions but also a little in the bulk melt. After approximately 4500 s, the sedimentation of equiaxed crystals mainly in the two corner regions became the dominant process, and progressively two crystals pileups formed. The motion of the sedimenting crystals appeared first quite straight but gradually got unsteady until at approximately 6800 s, large-scale vortices occurred that even transported crystal upwards again. At this stage, a noticeable rise in the interaction between the flow along the left and right cooled sidewalls was

observed. Figure 2 shows the flow field of both, liquid and equiaxed crystals. They are interconnected by drag; the sedimenting crystals also dragged the liquid downwards, and at the same time, the rising liquid moved, in particular, smaller crystals upwards. An elaborate description of the flow details of such experiments will be given in [14].

During stage 3 numerous sliding down of columnar segments occurred. Figure 3 illustrates three sections within the containment that were scrutinized at the appearance of this phenomenon. Figure 3a represents the uppermost section, followed by figure 3b, and finally figure 3c, with each section positioned successively below the preceding one. The segment in figure 3a descends towards the lower sections and so enters figure 3b and finally figure 3c. The collision of this segment with the lower columnar front results in further fragmentation. This process gives rise to a diverse range of fragments of varying sizes, as can be seen in figure 3c.

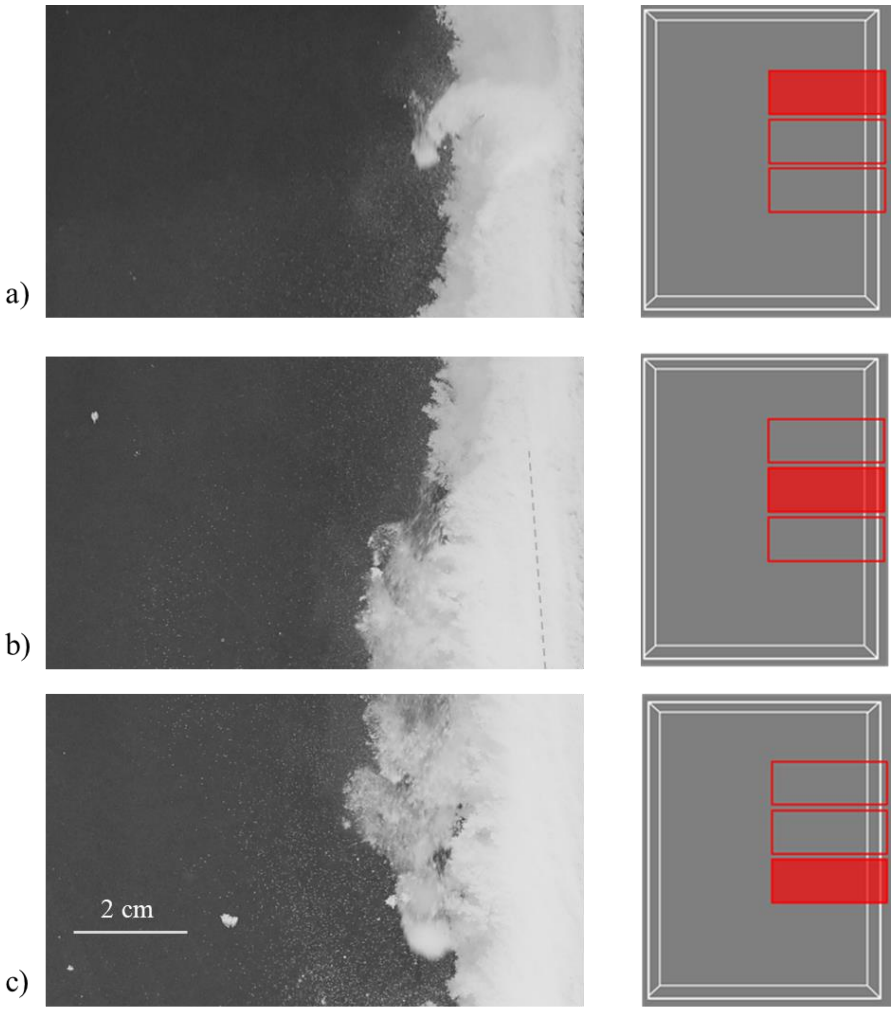

Figure 3. A crystal segment passes through the three indicted sections. The pictures were taken at a) $t = 8508$ s, b) $t = 8512$ s, c) $t = 8516$ s after the start of the cooling. The rolling down segment shown in a) is relatively small. Repetitive impact with the edge of the columnar mushy zone further fragments the segment so at in c) already a cloud of crystals is visible.

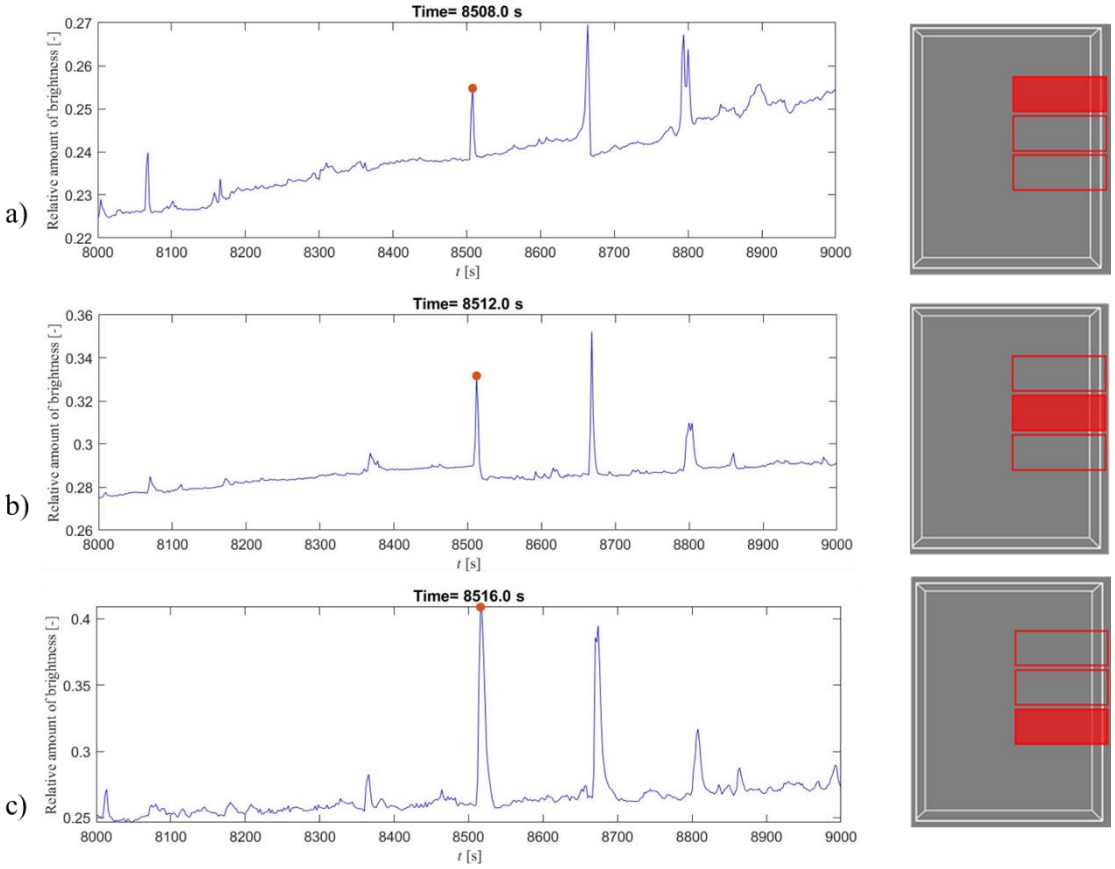

Figure 4. The image brightness of the three sections is shown in figure 3. The red dot indicates the moment when the corresponding pictures were recorded.

In figure 4, three peaks marked with red dots correspond to the distinct segment-sliding-down event identified in figure 3. Notably, in figure 4b and c, these peaks are observed with a time delay of 4 s. The brightness level is assessed by initially binarizing the grey level of each pixel, assigning either zero (white) or one (black), and then determining the proportion of 'white' pixels relative to the total number of pixels in the corresponding section. Consequently, the generally higher brightness in figure 4b, c compared to figure 4a indicates a greater amount of 'white' in the lower section compared to the section just above. The lower section consistently receives material from the upper columnar layers, while the upper section does not receive as much. The fragments entering a section are partially integrated into the existing columnar structure but predominantly continue to slide further downwards.

The experimental results presented here are not sufficient to directly prove the conditions that are necessary for the occurrence of detaching and sliding-down of columnar segments. However, since the pioneering work of Beckermann and Viskanta [15,16] it is well-known that the segregated melt in a dendritic ammonium chloride skeleton is less dense compared to the original liquid and thus rising solute buoyancy occurs. Such a flow scenario is intrinsically unstable and might lead to freckle formation [17, 18]. In the present case, the unsteady flow in the bulk melt leads to further destabilisation of the mushy zone flow as flow instabilities in the bulk melt penetrate into the edge of the columnar layer. As a consequence, flow channels that are inclined towards the interior of the containment transport segregated liquid to the edge of the columnar region. There, solidification is retarded and even melting might occur and thus columnar segments get detached. The inclined flow channel can be surmised in figure 3b) by the weak grey trace highlighted by the grey dotted line.

4. Conclusions

The following necessary conditions for the appearance of slighting-down columnar segments can be formulated: (i) a (mostly) vertical, large enough area of a columnar dendritic mushy zone must exist; (ii) the solid must have a higher density compared to the melt; (iii) interdendritic melt flow must locally change the solute concentration in the dendritic network such that further solidification is either retarded or even remelting occurs; (iv) the corresponding segment must be at the edge of the columnar dendritic mushy zone.

For the experimental conditions used in the present study, the interdendritic melt flow is caused by an upward solutal buoyancy within the dendritic network affected by the sedimentation of equiaxed crystals in the bulk melt. However, a straight upward flow in and a straight downward flow ahead of the mushy zone would not cause any change in the interdendritic solute concentration. For that to happen a horizontal flow component within the dendritic network is necessary. At the top of the solidifying liquid reservoir, the upward flow changes direction necessarily. However, instabilities in the upwards solutal-buoyancy flow also cause horizontal velocity components. These instabilities are known from the initialization of interdendritic flow channels and, in the present case, are fostered by unsteady vortices in the bulk melt ahead of the columnar mushy zone. After the sliding-down of a columnar segment, fragmentation of such a segment caused by a mechanical impact with lower mushy zone areas subsequently leads to a crystal multiplication and so an avalanche of crystals occurs.

The presented work demonstrates that our understanding of microstructure formation in larger castings must be completed by considering the formation of crystal avalanches and the corresponding occurrence of numerous further grains. Future numerical tools for microstructure predictions should account for this phenomenon, especially when applied to alloys that are prone to upward solutal buoyancy in the interdendritic mushy region.

References

[1] Kurz W, Fisher D J, Rappaz M 2023 *Fundamental of Solidification*, 5th ed. (Trans Tech Publications, Aedermansdorf)
[2] Thevoz P, Desbiolles J L and Rappaz M 1989 *Metall. Trans. A* **20** 311
[3] Campanella T, Charbon C, and Rappaz M. 2004 *Metall. Mater. Trans. A* **35** 3201
[4] Mathiesen R H, Arnberg L, Bleuet P and Somogyi A 2006 *Metall. Mater. Trans. A* **37** 15
[5] Kumar A and Dutta R 2008 *J. Phys. D* **41** 155501
[6] Hutt J and StJohn D 1998 *lnt. J. Cast Metals Res.* **11** 13
[7] Southin R T 1967 *Metall. Mater. Trans. A* **239** 22
[8] Wołczynski W 2016 in *The Encyclopedia of Iron, Steel, and Their Alloys*(Taylor & Francis Group, New York, 1910)
[9] Saffie M G M, Tan F L, and Tso C P 2013 *Therm. Eng.* **50** 562
[10] Ludwig A, Stefan-Kharicha M, Kharicha A, and Wu M 2017 *Metall. Mater. Trans. A* **48** 2927
[11] Kohn A 1977 *Int. Conf. Solidif. Cast.*, London Inst. Met., **1** 356
[12] Shayesteh G 2024 *On the Occurrence of Crystal Avalanches During Alloy Solidification* (Ph.D-Thesis, University of Leoben, Austria)
[13] Shayesteh G, Ludwig A, Stefan-Kharicha M, Wu M, and Kharicha A 2024 *Metall. Mater Trans. A* submitted
[14] Shayesteh G, Ludwig A, Stefan-Kharicha M, Kharicha A and Wu M 2024 *Int. J. Heat Mass Trans.* in preparation
[15] Beckermann C and Viskanta R 1988 *Int. J. Heat Mass Transfer* **31** 2077
[16] Beckermann C and Viskanta R 1989 *Chem. Eng. Comm.* **85** 135
[17] Sarazin J and Hellawell A 1988 *Metall. Mater. Eng.* **19** 1861
[18] Kumar A, Založnik M, Combeau H, Lesoult G, and Kumar A 2023 *Int. J. Heat Mass Trans.* **164** 120602